AD-A061 754 NORTHWESTERN UNIV EVANSTON ILL DEPT OF MECHANICAL E--ETC F/G 21/5
THERMOELASTIC AND DYNAMIC PHENOMENA IN SEALS.(U)
SEP 78 Y WU, R A BURTON N00014-75-C-0761
UNCLASSIFIED 5341-427-3 NL

1 OF 1
AD
A061754

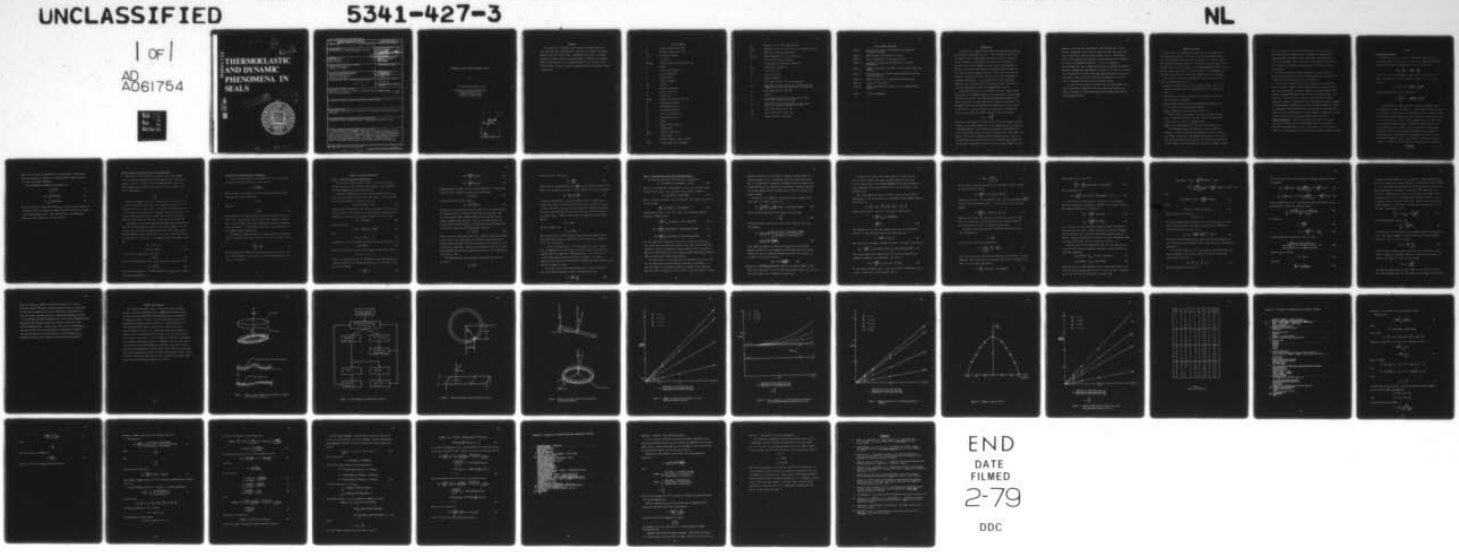

END
DATE
FILMED
2-79
DDC

12

LEVEL II

THERMOELASTIC AND DYNAMIC PHENOMENA IN SEALS

SECURITY CLASSIFICATION OF THIS PAGE (When Data Entered)

REPORT DOCUMENTATION PAGE

READ INSTRUCTIONS BEFORE COMPLETING FORM

1. REPORT NUMBER

2. GOVT ACCESSION NO.

3. RECIPIENT'S CATALOG NUMBER

4. TITLE (and Subtitle)
Thermoelastic and Dynamic Phenomena in Seals.

5. TYPE OF REPORT & PERIOD COVERED
Special Report
Jan~~uary 1978~~ - Sept~~ember~~ 1978

6. PERFORMING ORG. REPORT NUMBER
5341-427-3

7. AUTHOR(s)
Yih-Tsuen Wu
Ralph A. Burton

8. CONTRACT OR GRANT NUMBER(s)
N00014-75-C-0761
~~Mod. P00001~~

9. PERFORMING ORGANIZATION NAME AND ADDRESS
Northwestern University
Evanston, IL 60201

10. PROGRAM ELEMENT, PROJECT, TASK AREA & WORK UNIT NUMBERS

11. CONTROLLING OFFICE NAME AND ADDRESS
Procuring Contracting Officer
Office of Naval Research
Arlington, VA 22217

12. REPORT DATE
Sep~~tember 1~~978

13. NUMBER OF PAGES
46

14. MONITORING AGENCY NAME & ADDRESS (if different from Controlling Office)
12 45p.

15. SECURITY CLASS. (of this report)
Unclassified

15a. DECLASSIFICATION/DOWNGRADING SCHEDULE

16. DISTRIBUTION STATEMENT (of this Report)
Reproduction in whole or in part is permitted for any purpose of the United States Government.

DISTRIBUTION STATEMENT A
Approved for public release;
Distribution Unlimited

17. DISTRIBUTION STATEMENT (of the abstract entered in Block 20, if different from Report)

18. SUPPLEMENTARY NOTES
This report was presented as a MS Thesis to the Graduate School, Northwestern University.

19. KEY WORDS (Continue on reverse side if necessary and identify by block number)
lubrication, seals, tribology, failure, thermoelastic instability, wear

20. ABSTRACT (Continue on reverse side if necessary and identify by block number)
An analysis of a seal model is made where the rotating element has both fixed tilt and two-lobe waviness. The stator is assumed to be gimbal mounted and to have inertial mass. Hydrodynamic lubrication is assumed, following the short bearing or narrow seal model. Conditions are examined where the stator precesses in synchronism with the rotor rotation. Particular interest is given to operating conditions where such behavior appears to degenerate.

DD FORM 1 JAN 73 1473 EDITION OF 1 NOV 65 IS OBSOLETE

403502

SECURITY CLASSIFICATION OF THIS PAGE (When Data Entered)

THERMOELASTIC AND DYNAMIC PHENOMENA IN SEALS

by

Yih-Tsuen Wu and Ralph A. Burton

Department of Mechanical Engineering
and Astronautical Sciences
Northwestern University
Evanston, Illinois 60201

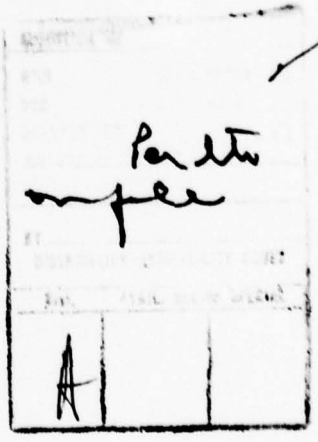

ABSTRACT

An analysis of a seal model is made where the rotating element has both fixed tilt and two-lobe waviness. The stator is assumed to be gimbal mounted and to have inertial mass. Hydrodynamic lubrication is assumed, following the short bearing or narrow seal model. Conditions are examined where the stator precesses in synchronism with the rotor rotation. Particular interest is given to operating conditions where such behavior appears to degenerate.

LIST OF SYMBOLS

A	variable defined by Eq. (61)
B	variable defined by Eq. (62)
C_1, C_2	integration constant
f	face load
$F(\Phi_1, \Phi_2)$	function of Φ_1, Φ_2 defined by Eq. (55)
g	gravity
h	overall film-thickness
$\bar{h}$	mean film-thickness
h_o	operating wave
I	moment of inertia
INT	integral
K	thermal conductivity
L	width of face seal
$\tilde{m}$	stator mass
M_X, M_Y	moment about X,Y axes [Fig. (4)]
N	revolutions per minute
p	hydrodynamic pressure
$\bar{p}$	seal width-averaged p
q	overall viscous heating
q'	non-uniform heating
R	radius
u	fluid velocity function
V	sliding speed
V_{crit}	critical sliding speed
$\tilde{w}$	stator weight
x	distance along the edge of contact
X,Y,Z	rotating cartesian coordinates

z_1'	amplitude of first mode operating wave
$\hat{z}_1, \hat{z}_2$	amplitude of first, second mode of rotor operating waviness
$\tilde{z}_1$	amplitude of stator operating wave
$\hat{z}_{1i}, \hat{z}_{2i}$	initial amplitude of $\hat{z}_1$, $\hat{z}_2$ on the rotor
α	coefficient of thermal expansion
γ	tilting angle of the stator in operation
δ_{th}	thermoelastic deformation
ϵ	ratio of $\hat{z}_2$ to $\bar{h}$
ζ	ratio of z_1' to $\hat{z}_2$
θ	angular coordinate
λ	phase angle defined by Eq. (3) of Appendix B
ϕ_1	phase angle of first mode of rotor operating waviness relative to rotating coordinates [Fig. (4) & Eq. (15)]
ϕ_2	phase angle defined in Eq. (29)
μ	viscosity
Φ_1	phase angle of first mode operating wave relative to rotating coordinates [Eq. (16)]
ψ_1	phase angle of initial first mode of rotor waviness relative to rotating coordinates [Eq. (51)]
ψ_2	phase angle defined in Eq. (52)
$\Delta\psi_i$	phase angle defined in Eq. (57)
ω	angular velocity of the rotor

LIST OF FIGURES AND TABLE

INTRODUCTION

In recent years, numerous theories have been advanced to investigate the mechanism of mechanical face seal. It is now widely accepted that misalignment alone or coupled with seal surface waviness is the cause for the existence of a lubricating fluid film between seal faces. In the case of non-flexible mounted face seal, while stable operation is possible if only one of the surfaces is misaligned, Harrdt & Godet [1] have shown that axial vibration may occur if both of the faces are misaligned. Flexibly mounted face seals are used in many applications to accomodate misalignment. These should have at least second mode waviness on one of the surfaces in order to have stable motion has been stated and experimentally proved by Stanghan-Batch & Iny [2].

Thin film flows between solid boundaries can cause viscous heating which may lead to thermal deformation of the solid surface and consequent alterations in the flow. The heating and deformation may enhance each other progressively to cause large surface distortions and failure. The phenomenon, referred to as "Thermoelastic Instability" has been studied by Banerjee [3]. Critical sliding speed, above which instability may occur, has been found, for thermal conductor sliding on insulator:

$$V_{crit} = \bar{h}\kappa\sqrt{\frac{K}{\mu\alpha}} \qquad (1)$$

where mean film-thickness $\bar{h}$ is held fixed, κ is the wave number of the disturbance, K the thermal conductivity of the conductor and α its coefficient of thermal expansion. The critical speeds measured experimentally were found to match those predicted by Eq. (1) extremely well. This equation is, however, restricted to constant $\bar{h}$ and non-flexible mounting. Later, an improved model where constant $\bar{h}$ condition is relaxed has been studied [4], finding that thermoelastic effects lead to a continuous change in surface

waviness as well as mean film-thickness, with changing speed. Consequently, the unstable region cannot be obtained in practice because there exists no path to it from the initial waviness at rest. This theory is based on the assumption that mounting is inertialess therefore eliminates the effect of misalignment completely. In a set of experiments later performed [5], where a gimbal has been used to simulate the flexible mounting, although mean film-thickness is predicted very well by the theory, it is observed that first mode wave grows almost three-fold in the tested speed range. This increase is believed to be thermoelastic in nature, and is a consequence of gimbal inertia, loading the faces.

In view of the above fact, a new model for the flexible mounted face seal is studied here, taking both first and second mode waviness into account, to provide a better understanding of its dynamic characteristic and thermoelastic effect.

METHOD OF APPROACH

A three degree of freedom face seal model has been proposed which is illustrated in Fig. (1). The "rotor" is a floating element with both first and second mode waviness on the seal surface; the "stator" is flexibly mounted such that the edge of its flat surface can have angular displacement about its center of mass. It is also assumed that rotor is a good thermal conductor while stator is a good insulator. This assumption is reasonable [6] and leads to considerable simplification of the analysis.

The procedure for solving the problem can then be stated as follows: [refer to block diagram, Fig. (2)]

1. Assuming that film stiffness largely insures tracking, that is, the stator will follow the rotor synchronously (but not necessarily in phase).
2. Considering steady state solutions only and choosing the most convenient rotating coordinates.
3. Assuming small-perturbations, thus allowing hydrodynamic pressure to be a linear function of operating waviness.

   Case 1. Removing second mode waviness from rotor.

   This enables one to calculate the force and moment integrals. This is examined to see what is the role of the first mode film-thickness when the stator is flexibly mounted.

   Case 2. The configuration where first and second modes exist.

   The information previously obtained is used to simplify the analysis. It will be found that the problem can still be treated as a linear one where force and moment depend "seperately" on second mode and first mode operating waviness, so long as waviness amplitude is small compared with film-thickness. Once force and moment integrals

have been carried out, one can easily arrive at the last step of the block diagram, where operating waves are composed of initial waviness and thermoelastic deformation on the rotor, plus stator tilt which is caused by hydrodynamic forces. Use of this result enables one to obtain the condition of thermoelastic instability, and to find out critical sliding speed.

When the restriction of small-perturbation is removed, it will be shown that the characteristics of the problem remain the same while only a numerical correction factor need to be considered.

Reiterating, the motion of face seal elements will be investigated, where the rotor is rigidly fixed to a shaft, and may be tilted as well as wavy in the second mode. It will be treated as a thermal conductor and subject to thermal deformation as the result of frictional heating by the fluid film. The stator will be treated as a flat, thermal insulator supported in gimbals. Operation will be studied where the waviness component of film-thickness is small relative to the mean value (a condition observed in experiments), and particular interest will be given to those operating conditions where this configuration becomes impossible. Hydrostatic pressure and leakage effects will be omitted from the present analysis.

Comment on Notation. In that which follows the tilda ($\tilde{}$) will denote quantities associated with the stator and the carat ($\hat{}$) will denote quantities associated with the rotor. First mode or tilt of the stator would be, in such notation, $\tilde{x} \cos \theta$, when θ is a measure of angular position.

THEORY

Hydrodynamic equations:

Referring to Fig. (3), it will be assumed that radius R is much larger than width L of seal surface, therefore a one dimensional Reynold's equation with narrow-face approximation [7] can be written as

$$\frac{\partial}{\partial y}\left(h^3 \frac{\partial p}{\partial y}\right) = 6V\frac{\partial h}{\partial x} + 12\frac{\partial h}{\partial t} \tag{2}$$

where h is overall film-thickness, a function of x and t but not of y. Hence, integrating p twice with boundary conditions $p = 0$ at $y = \pm L/2$ results in

$$p = \left(\frac{1}{2}y^2 - \frac{1}{8}L^2\right)\left(\frac{6\mu V}{h^3}\frac{\partial h}{\partial x} + \frac{12\mu}{h^3}\frac{\partial h}{\partial t}\right) \tag{3}$$

Width-averaged pressure can be calculated as

$$\bar{p} = \frac{1}{L}\int_{-\frac{L}{2}}^{\frac{1}{2}} p\,dy = -\frac{\mu V L^2}{2h^3}\frac{\partial h}{\partial x} - \frac{\mu L^2}{h^3}\frac{\partial h}{\partial t} \tag{4}$$

Rotating coordinates may be chosen to simplify the problem. Under the assumption of synchronous motion, it can be recognized that the pressure distribution is rotating wave, but non-varying in shape; therefore it will be convenient to choose moving coordinates such that pressure function will be fixed with respect to them. In this favorable reference frame system, the film-thickness wave is fixed. This does not require that the wave representing tilt of the rotor or stator to be in phase with the film-thickness, but only that the phase relationships in the ensemble are preserved in time. Recall that the surface waves are fixed to the rotor, hence $\partial h/\partial t$ disappears, and the stator surface is moving past with the velocity -V. When this sign is taken into account Eq. (4) is replaced by

$$\bar{p} = \frac{\mu V L^2}{2h^3}\frac{\partial h}{\partial x} \tag{5}$$

where V is now simply the magnitude of the sliding speed. This equation shows that pressure is a function of position and that squeeze effect is not seen in the chosen coordinates.

Force and moment, according to definitions, are

$$f = \int_{p^+} \bar{p} LR d\theta \tag{6}$$

$$M_X = -\int_{p^+} \bar{p} LR^2 \sin\theta d\theta \tag{7}$$

$$M_Y = \int_{p^+} \bar{p} LR^2 \cos\theta d\theta \tag{8}$$

where "p^+" is used to denote that integrals are effective only when pressure is positive, while in the region of negative pressure cavitation is assumed to occur and pressure is zero. This condition has been experimentally proved to be quite accurate for the face seal [2].

Motion of stator and definition of rotating coordinates

When seal is steadily operating at certain speed, hydrodynamic force is constant in amplitude but moving along the edge of the stator surface. It can be seen that if the tilting amplitude $\tilde{z}_1$ (Fig. 4) is small compared with R, which is generally true, then the angle of tilt will be approximately:

$$\gamma = \frac{\tilde{z}_1}{R} \tag{9}$$

Rotating coordinates (see Fig. 4) may be chosen so that the y axis is the axis about which tilt occurs, and it may also be taken to lie in the plane of the face of the stator. The x axis is perpendicular to the y axis and points in the direction of maximum elevation of the stator. The Z axis is that about which the rotor turns and is taken to be vertical, while the z axis represents the normal to the plane of the stator face.

The dynamics of an axially symmetric mass moving with such an Eulerian frame are well understood (see Appendix F for further comment). For the case where the tilt angle γ (measured between the z and Z axes) retains constant magnitude, while the direction of the y axis rotates steadily at the angular speed of the shaft, ω, the moments acting on the mass are such that

$$M_x = 0, \; M_z = 0$$

$$M_y = I\omega^2 \sin\gamma\cos\gamma \tag{10}$$

If the stator is taken to be a thin ring

$$I = \tilde{m}R^2/2 \tag{11}$$

where R is the mean radius of the ring, and Eq. (10) becomes, for small γ

$$M_y = \frac{\tilde{m}}{2}\frac{V^2}{R}\tilde{z} \tag{12}$$

Recall that this moment is of constant magnitude and always acts to oppose the angular displacement γ.

Heating effect and thermoelastic deformation

It has been shown [8] that for incompressible flow in thin films, viscous heat generated within the film is given by

$$q = \int_0^h \mu \left(\frac{\partial u}{\partial z}\right)^2 dz$$

Under the short bearing model, the fluid velocity distribution in the film approaches Couette flow which is

$$u = V\frac{z}{h}$$

therefore

$$q = \frac{\mu V^2}{h} \tag{13}$$

Georgopoulos [9] has found that under typical seal conditions convected heat is only a small amount of percentage of that conducted. In view of this it can be assumed that generated heat will be removed by conduction alone, furthermore, it would conduct totally into the rotor which is the only conductor under consideration.

The equation relating heat input to a surface and the corresponding surface curvature has been shown by Burton et al [10], and will be written as

$$\frac{d^2\delta_{th}}{dx^2} = \frac{\alpha q'}{K} \tag{14}$$

where δ_{th} means the thermoelastic deformation on the rotor surface, and q' is non-uniform part of total heating q since uniform heating can only lead to zero curvature.

ANALYSIS FOR SMALL-PERTURBATION

Case 1. Rotor has only first mode waviness

In this case, we shall examine whether a steady state solution is possible when there exists only first mode waviness, and its amplitude very small compared with mean film-thickness $\bar{h}$.

Overall film-thickness is the sum of $\bar{h}$ and the operating wave h_o, where h_o comes from rotor waviness and stator motion. To be consistent with chosen coordinates, it will be written as

$$h_o = \hat{z}_1 \sin(\theta+\phi_1) - \tilde{z}_1 \cos\theta \tag{15}$$

where $\hat{z}_1$ denotes amplitude of rotor waviness, $\tilde{z}_1$ amplitude of the stator and ϕ_1 is a phase angle determined by initial waviness and thermoelastic deformation. For convenience, h_o may be simplified into one term as

$$h_o = z_1' \sin(\theta+\Phi_1) \tag{16}$$

with the relation

$$z_1' = (\hat{z}_1^2 - 2\hat{z}_1\tilde{z}_1 \sin\phi_1 + \tilde{z}_1^2)^{\frac{1}{2}} \tag{17}$$

and

$$z_1' \sin\Phi_1 = \hat{z}_1 \sin\phi_1 - \tilde{z}_1 \tag{18}$$

Recalling Eq. (5) and noting that positive pressure implies $dh/d\theta > 0$, or

$$z_1' \cos(\theta+\Phi_1) > 0 \tag{19}$$

Therefore the positive pressure region around the seal surface will be

$$-\frac{\pi}{2} - \Phi_1 < \theta < \frac{\pi}{2} - \Phi_1$$

With use of this interval and the assumption of small amplitude waviness (such that $z_1'/\bar{h} \ll 1$), the following results can be easily derived from Eq. (6), (7) and (8)

$$f = \frac{\mu V L^3}{\bar{h}^3} z_1' \tag{20}$$

$$M_X = \frac{\pi\mu V L^3 R}{4\bar{h}^3} z_1' \sin\Phi_1 \tag{21}$$

$$M_Y = \frac{\pi\mu V L^3 R}{4\bar{h}^3} z_1' \cos\Phi_1 \tag{22}$$

Remembering $M_X = 0$ and $M_Y > 0$ for the chosen coordinates, it follows that Φ_1 must be zero. With this constraint, Eq. (18) becomes

$$\tilde{z}_1 = \hat{z}_1 \sin\phi_1 \tag{23}$$

inserting this into Eq. (17) yields

$$z_1' = \sqrt{\hat{z}_1^2 - \tilde{z}_1^2}\, \sin\theta \tag{24}$$

Physically $\Phi_1 = 0$ means the stator will follow (tilt) in a way such that the operating wave h_o is 90^o out of phase with the stator wave. The generated pressure will be symmetric about X axis, therefore it will produce no moment about this axis. Also it is observed from Eq. (23) that $\tilde{z}_1$ should be smaller than $\hat{z}_1$. Consider the special situation, where the stator is fixed, then the operating wave reduces to

$$h_o = \hat{z}_1 \sin\theta \tag{25}$$

which is the case investigated earlier [4]. Another limiting case happens when $\hat{z}_1 = \tilde{z}_1$, it turns out that $\phi_1 = \pi/2$ and $z_1' = 0$ which means stator keeps parallel with rotor, obviously no pressure will be generated in this position hence impossible. Nevertheless it points out that if z_1' is very small compared with $\hat{z}_1$, then $\tilde{z}_1$ approaches $\hat{z}_1$ and there is a slight phase shift from $\phi_1 = \pi/2$.

The relation between force and moment derived from Eq. (20) and Eq. (22) is

$$M_Y = \frac{R\pi}{4} f$$

inserting into Eq. (12) yields

$$\tilde{z}_1 = \frac{\pi R^2}{2\tilde{m}V^2} f \tag{26}$$

Rewrite this by changing $\tilde{m}$ to $\tilde{w}/g$, and $\frac{60V}{2\pi R} = N$, where $\tilde{w}$ is the weight of the stator, N is revolutions per minute, and it becomes, after some rearrangement

$$\tilde{z}_1 = \left(\frac{g}{8\pi}\right) \left(\frac{f}{\tilde{w}}\right) \left(\frac{60}{N}\right)^2 \tag{27}$$

In general the axial load f is not necessarily related to stator weight. In this case, however, we may assume that axial load is equal to the weight of the rotor and be consistent with the experiment previously performed. It is then found that $\tilde{z}_1$ will be too large even for relatively high speed. For example, take $f = 10\tilde{w}$, N = 3000 r.p.m., tilt amplitude will be approximately

$$\tilde{z}_1 = 1.5\text{mm}$$

and for N = 1000 r.p.m.,

$$\tilde{z}_1 = 13.75\text{mm}$$

But as stated before, steady operation requires $\hat{z}_1$ always bigger than $\tilde{z}_1$ which means initial waviness should have at least same order of amplitude as $\tilde{z}_1$, and is impractical.

It can be concluded that for a flexible mounted face seal, if axial force is comparable with stator weight, then there will be no steady state solution under the assumption of synchronous motion. The reason lies in the fact that single wave provide both force and moment. The moment required by the stator is very small while the moment generated is large if same wave has to support the load.

Returning to Eq. (27) and requiring $\tilde{z}_1 = \hat{z}_1$, one finds the limiting speed below which operation is strictly forbidden, this being

$$N^2 = \frac{(60)^2}{8\pi} \frac{fg}{\tilde{w}\hat{z}_1} \tag{28}$$

Case 2. Rotor has both first and second mode waviness

The operating film wave in this case can be expressed as

$$h_o = \hat{z}_1 \sin(\theta+\phi_1) + \hat{z}_2 \sin(2\theta+\phi_2) - \tilde{z}_1 \cos\theta \tag{29}$$

where $\hat{z}_2$ is the amplitude of second mode on rotor, ϕ_2 is the phase angle relative to the stator. As in previous cases, it can be reduced to

$$h_o = z_1' \sin(\theta+\Phi_1) + \hat{z}_2 \sin(2\theta+\phi_2) \tag{30}$$

where z_1' and Φ_1 are defined in Eq. (17) and (18). The condition of positive pressure becomes

$$\frac{dh}{d\theta} = z_1' \cos(\theta+\Phi_1) + 2\hat{z}_2 \cos(2\theta+\phi_2) > 0 \tag{31}$$

Assuming again $h_o/\bar{h} \ll 1$, amd $1/h^3 \approx 1/\bar{h}^3$, force and moment equations assume the following forms

$$f = \frac{\mu V L^3}{2\bar{h}^3} \int_{p^+} [z_1' \cos(\theta+\Phi_1) + 2\hat{z}_2 \cos(2\theta+\phi_2)]d\theta \tag{32}$$

$$M_X = \frac{-\mu V L^3 R}{2\bar{h}^3} \int_{p^+} [z_1' \cos(\theta+\Phi_1) + 2\hat{z}_2 \cos(2\theta+\phi_2)]\sin\theta d\theta \tag{33}$$

$$M_Y = \frac{\mu V L^3 R}{2\bar{h}^3} \int_{p^+} [z_1' \cos(\theta+\Phi_1) + 2\hat{z}_2 \cos(2\theta+\phi_2)]\cos\theta d\theta \tag{34}$$

Eq. (31) shows that integration interval p^+ is a function of z_1', $\hat{z}_2$, Φ_1 and ϕ_2, therefore the analytical treatment of Eq. (32), (33) and (34) seems impossible. However, conclusions from the previous case and the symmetric property of second mode can be used to make reasonable simplifying assumption which will make closed form solution possible.

As stated before, if first mode alone is responsible for the face load, then the moment generated will usually be too much for equilibrium. In order that moment be of reasonable magnitude, one must let z_1' become very small such that it is unable to lift the load. On the other hand, the second

mode has the ability to lift load while producing no moment owing to its symmetric property. So in the combined case of first mode plus second mode, it is reasonable to assume that z_1' should be very much smaller than second mode waviness $\hat{z}_2$, such that the second mode is largely responsible for the load support and the first mode wave is small but sufficient for dynamic tracking.

To prove the above argument, recalling the dynamic equation of the stator again, it becomes, for this case

$$\tilde{z}_1 = \frac{R^2}{\tilde{m}V^2} \frac{\mu V L^3}{\bar{h}^3} \hat{z}_2 \int_{p+} \left[\frac{z_1'}{\hat{z}_2}\cos(\theta+\phi_1) + 2\cos(2\theta+\phi_2)\right]\cos\theta d\theta \qquad (35)$$

where Φ_1 and ϕ_2 must satisfy condition $M_X = 0$. By defining

$$\zeta = \frac{z_1'}{\hat{z}_2} \qquad (36)$$

and substituting Eq. (32) into Eq. (35) it will result in, after some rearrangement,

$$\tilde{z}_1 = \left(\frac{g}{2\pi^2}\right)\left(\frac{f}{\tilde{w}}\right)\left(\frac{60}{N}\right)^2 \frac{\int_{p+} \left[\zeta\cos(\theta+\Phi_1) + 2\cos(2\theta+\phi_2)\right]\cos\theta d\theta}{\int_{p+} \left[\zeta\cos(\theta+\Phi_1) + 2\cos(2\theta+\phi_2)\right]d\theta}$$

$$= \left(\frac{g}{2\pi^2}\right)\left(\frac{f}{\tilde{w}}\right)\left(\frac{60}{N}\right)^2 \left(\frac{INT(M)}{INT(F)}\right) \qquad (37)$$

where INT(M) and INT(F) are notations for moment and force integrals. Computer results [Fig. (5) & Appendix A] indeed show that ζ must be much smaller than unity to keep $\tilde{z}_1$ within practical range. For instance, if N = 3000 r.p.m. and $f/\tilde{w} = 10$, then

$$\tilde{z}_1 \approx 10.2 * \left(\frac{INT(M)}{INT(F)}\right) \qquad \text{(cm)}$$

for $\tilde{z}_1 \leq 2.5 \times 10^{-3}$ (cm), INT(M)/INT(F) should be less than $1.25*10^{-2}$. From Fig. (5) one finds that $\zeta < 0.1$ (for any possible phase angle) or $z_1' < 0.1\ \hat{z}_2$. And for N = 1000 r.p.m., ζ should be less than 0.01.

As shown before, small ζ which implies small z_1' ($= \zeta\hat{z}_2$) will mean that the stator follows in the position almost parallel to the rotor. It can be expected that if the stator approaches the inertialess condition then z_1' approaches zero and second mode will be the only waviness in the operating film.

Under the assumption of small ζ, positive region can be determined approximately by only second mode since first mode can only slightly change it. Hence p^+ will be

$$-\frac{\pi}{4} - \frac{\phi_2}{2} < \theta < \frac{\pi}{4} - \frac{\phi_2}{2} \text{ and } \frac{3\pi}{4} - \frac{\phi_2}{2} < \theta < \frac{5\pi}{4} - \frac{\phi_2}{2}$$

Assuming that $h_o/\bar{h} \ll 1$, and $\zeta \ll 1$, force will be approximately

$$f = \frac{\mu V L^3}{2\bar{h}^3}\hat{z}_2 \int_{p^+} 2\cos(2\theta+\phi_2)d\theta$$

$$= \frac{2\mu V L^3}{\bar{h}^3}\hat{z}_2 \qquad (38)$$

this equation fits very well with numerical data [Fig. (6) and Appendix A with $\epsilon = 0$]. Mean film-thickness can be derived from it as

$$\bar{h} = \left(\frac{2\mu V L^3}{f}\right)^{1/3} (\hat{z}_2)^{1/3} \qquad (39)$$

With same kind of reasoning, the moment can also be calculated. From Eq. (33)

$$M_X = \frac{-\mu V L^3 R}{2\bar{h}^3}\left\{\int_{p^+} z_1'\cos(\theta+\Phi_1)\sin\theta d\theta + \int_{p^+} 2\hat{z}_2\cos(2\theta+\phi_2)\sin\theta d\theta\right\} \qquad (40)$$

The second integral can be equated directly to zero by recognizing the symmetrical property of the second mode, the result is

$$M_X = \frac{-\mu V L^3 R}{2\bar{h}^3} z_1'\left\{\sin(\Phi_1-\phi_2) - \frac{\pi}{2}\sin\Phi_1\right\} \qquad (41)$$

For the chosen coordinates, $M_X = 0$, hence there exists a relationship between Φ_1 and ϕ_2, which can be derived from Eq. (41) as

$$\tan\Phi_1 = \frac{\sin\phi_2}{\cos\phi_2 - \frac{\pi}{2}} \tag{42}$$

with the above restriction, M_Y will be the total moment, which if follows the same procedures as M_X did

$$M_Y = \frac{\mu V L^3 R}{2\bar{h}^3} z_1' \left\{\cos(\Phi_1-\phi_2) + \frac{\pi}{2}\cos\Phi_1\right\} \tag{43}$$

Computer results [Fig. (7) and Appendix A] show that the total moment $\sqrt{M_X^2+M_Y^2}$ is accurate even when ζ approaches 0.5. From Eq. (12), tilt of the stator becomes

$$\tilde{z}_1 = \frac{\mu R^2 L^3}{2\tilde{m}V\bar{h}^3} z_1' \left\{\cos(\Phi_1-\phi_2) + \frac{\pi}{2}\cos\Phi_1\right\} \tag{44}$$

Equation (39) and (44) show that mean film-thickness depends on second mode only, and tilt of the stator depends on first mode wave amplitude alone but will be affected by second mode position (ϕ_2).

Heating effects and thermoelastic deformations will now be dealt with. Recalling that

$$q = \frac{\mu V^2}{h}$$

when $h_o \ll \bar{h}$, it will become approximately

$$q = \frac{\mu V^2}{\bar{h}(1+\frac{h_o}{\bar{h}})} = \frac{\mu V^2}{\bar{h}} - \frac{\mu V^2}{\bar{h}^2} h_o \tag{45}$$

where first term is the uniform heating which does not contribute to surface curvature. The second term is non-uniform heating caused by operating film wave. It can be further expressed as

$$q' = \frac{-\mu V^2}{\bar{h}^2}\left\{z_1'\sin(\theta+\Phi_1) + \hat{z}_2\sin(2\theta+\phi_2)\right\} \tag{46}$$

Substituting into Eq. (14) yields

$$\frac{d^2\delta_{th}}{dx^2} = \frac{-\alpha\mu V^2}{K\bar{h}^2}\left\{z_1'\sin(\theta+\phi_1) + \hat{z}_2\sin(2\theta+\phi_2)\right\} \tag{47}$$

After integrating twice,

$$\delta_{th} = \frac{\alpha\mu V^2 R^2}{K\bar{h}^2}\left\{z_1'\sin(\theta+\phi_1) + \frac{\hat{z}_2}{4}\sin(2\theta+\phi_2)\right\} + C_1\theta + C_2 \tag{48}$$

Clearly, both C_1 and C_2 should be zero because of seal geometry. Therefore thermoelastic deformation is composed of first mode and second mode component which will be expressed as

$$\delta_{th_1} = \frac{\mu\alpha V^2 R^2}{K\bar{h}^2} z_1'\sin(\theta+\phi_1) \tag{49}$$

$$\delta_{th_2} = \frac{\mu\alpha V^2 R^2}{4K\bar{h}^2} \hat{z}_2\sin(2\theta+\phi_2) \tag{50}$$

It is noted that the above derivation implicitly assumes that heating is generated by the full film. Stanghan-Batch [2] has shown that although cavitated regions exist, the fluid is partially continuous around seal surface. Therefore actual values of heating and surface deformation should lie between the extremes, full film and absent film when p = 0.

Referring to the block diagram again [Fig. (2)], two equations can be written from initial and operating conditions by separating first and second mode components

$$\hat{z}_{1i}\sin(\theta+\psi_1) + \delta_{th_1} - \tilde{z}_1\cos\theta = z_1'\sin(\theta+\phi_1) \tag{51}$$

$$\hat{z}_{2i}\sin(2\theta+\psi_2) + \delta_{th_2} = \hat{z}_2\sin(2\theta+\phi_2) \tag{52}$$

where $\hat{z}_{1i}$, $\hat{z}_{2i}$ are initial amplitude of first, second mode waviness of the rotor, ψ_1 and ψ_2 are phase angles relative to the stator wave. Substitute Eq. (43, 49, 50) into Eq. (51) and Eq. (52) which yield

$$\hat{z}_{1i}\sin(\theta+\psi_1) = z_1' \left\{1 - \frac{\mu\alpha V^2 R^2}{K\bar{h}^2}\right\}\sin(\theta+\Phi_1) + \tilde{z}_1\cos\theta$$

$$= \tilde{z}_1 \left\{\frac{\tilde{\ell}\, m V \bar{h}^3}{F(\Phi_1,\Phi_2)\mu R^2 L^3}\left[1 - \frac{\mu\alpha V^2 R^2}{K\bar{h}^2}\right]\sin(\theta+\Phi_1) + \cos\theta\right\} \quad (53)$$

and

$$\hat{z}_{2i}\sin(2\theta+\psi_2) = \hat{z}_2 \left\{1 - \frac{\mu\alpha V^2 R^2}{4K\bar{h}^2}\right\}\sin(2\theta+\Phi_2) \quad (54)$$

where

$$F(\Phi_1,\Phi_2) = \cos(\Phi_1-\Phi_2) + \frac{\pi}{2}\cos\Phi_1 \quad (55)$$

From Eq. (54) it is found that

$$\psi_2 = \Phi_2 \pm 2\pi$$

which means thermoelastic deformation in the second mode will be in phase with the initial waviness. Operating waviness $\hat{z}_2$ can be obtained by substituting Eq. (39) into Eq. (54) as

$$\hat{z}_{2i} = \hat{z}_2 - \frac{\mu\alpha V^2 R^2}{4K}\left(\frac{2\mu V L}{f}\right)^{-2/3}(\hat{z}_2)^{1/3} \quad (56)$$

Therefore if initial amplitude $\hat{z}_{2i}$ is known, then operating amplitude $\hat{z}_2$ can be determined and will depend on load, sliding speed and other physical properties.

The initial conditions of the rotor waviness including amplitude and phase relationship. Phase shift between first mode and second mode waviness will be defined by

$$\Delta\psi_i = \frac{\psi_2}{2} - \psi_1 = \frac{\Phi_2}{2} - \psi_1 \pm \pi \quad (57)$$

where $\Delta\psi_i$ ranges from $-\pi/2$ to $\pi/2$.

Inserting this into Eq. (53) and taking two orthogonal components yields two equations

$$\hat{z}_{1i}\cos\left(\frac{\phi_2}{2}\pm\pi-\Delta\psi_i\right) = \tilde{z}_1\left[\frac{2\tilde{m}V\bar{h}^{-3}}{\mu R^2 L^3 F(\Phi_1,\phi_2)}\left(1-\frac{\mu\alpha V^2R^2}{K\bar{h}^{-2}}\right)\right]\cos\Phi_1 \tag{58}$$

$$\hat{z}_{1i}\sin\left(\frac{\phi_2}{2}\pm\pi-\Delta\psi_i\right) - \tilde{z}_1 = \tilde{z}_1\left[\frac{2\tilde{m}V\bar{h}^{-3}}{\mu R^2 L^3 F(\Phi_1,\phi_2)}\left(1-\frac{\mu\alpha V^2R^2}{K\bar{h}^{-2}}\right)\right]\sin\Phi_1 \tag{59}$$

where ϕ_2 ranges from $-\pi$ to π. Recalling Eq. (42) which relates Φ_1 to ϕ_2, and dividing Eq. (59) by Eq. (58) will yield

$$\frac{\tilde{z}_i}{\hat{z}_{1i}} = \frac{\frac{\pi}{2}\sin\left(\frac{\phi_2}{2}\pm\pi-\Delta\psi_i\right) + \sin\left(\frac{\phi_2}{2}\pm\pi+\Delta\psi_i\right)}{\frac{\pi}{2} - \cos\phi_2} \tag{60}$$

By defining

$$A = \frac{2\tilde{m}V\bar{h}^{-3}}{\mu R^2 L^3} \tag{61}$$

$$B = 1 - \frac{\mu\alpha V^2R^2}{K\bar{h}^{-2}} = 1 - \left(\frac{V}{V}\right)^2_{crit} \tag{62}$$

and substituting Eq. (60) into Eq. (58), one finds

$$\frac{\cos\left(\frac{\phi_2}{2}\pm\pi-\Delta\psi_i\right)\left(\frac{\pi}{2}-\cos\phi_2\right)F(\Phi_1,\phi_2)}{\left[\frac{\pi}{2}\sin\left(\frac{\phi_2}{2}\pm\pi-\Delta\psi_i\right) + \sin\left(\frac{\phi_2}{2}\pm\pi+\Delta\psi_i\right)\right]\cos\Phi_1} = AB \tag{63}$$

Also Eq. (44) now becomes

$$\tilde{z}_1 = \frac{F}{A}\,z_1' \tag{64}$$

therefore

$$\frac{z_1'}{A\hat{z}_{1i}} = \frac{\tilde{z}_1}{\hat{z}_{1i}F(\Phi_1,\phi_2)} \tag{65}$$

A computer program [Appendix D] has been written to evaluate AB and $z_1'/A\hat{z}_{1i}$. Part of the results, where negative $\tilde{z}_1/\hat{z}_{1i}$ is not allowed, are shown in Table 1. It is found that AB may have positive and negative values for any initial phase angles, and is zero when $\tilde{z}_1 = \hat{z}_{1i}$ and $\psi_1 = 90^o$, which means z_1' is restricted. Although this is true, it is also found that $z_1'/A\hat{z}_{1i}$ reaches maximum (when $\Delta\psi_i = 0^o$) or near maximum (for other $\Delta\psi_i$) at AB = 0. Values of $z_1'/A\hat{z}_{1i}$ for AB = 0 are shown in Fig. (6). Whether these values can be reached depends on A. For example, take the worst case when $\Delta\psi_i = 0^o$, Fig. (8) shows that $z_1'/A\hat{z}_{1i} = 1.75$, so

$$\frac{z_1'}{\hat{z}_{1i}} = \underset{B=0}{(1.75A)} = 3.5\,\frac{\tilde{m}V_{crit}\bar{h}^3}{\mu R^2 L^3} \tag{66}$$

By substituting for $\bar{h}$ from Eq. (39),

$$\frac{z_1'}{\hat{z}_{1i}} = \frac{7\tilde{m}V^2_{crit}}{fR^2}\,\hat{z}_2 \tag{67}$$

A limiting case is that $\tilde{m}$ becomes very large (approaching the fixed mounting case), then z_1' will approach infinity, which is the case investigated earlier [1]. Eq. (67) can be changed to

$$V^2_{crit} = \frac{fR^2}{7\tilde{m}}\,\frac{z_1'}{\hat{z}_{1i}\hat{z}_2} \tag{68}$$

Since the stable condition requires $z_1' \ll \hat{z}_2$, it is instructive to choose values of $z_1'/\hat{z}_2$ as the limiting condition to evaluate critical speed. For instance, if $z_1'/\hat{z}_2 = 0.1$, then Eq. (68) becomes

$$V^2_{crit} = \frac{fR^2}{70\tilde{m}\hat{z}_{1i}}$$

The ranges of f,R,$\tilde{m}$ and $\hat{z}_{1i}$ may vary broadly for face seals, and so will the critical sliding speed. Eq. (69) points out that bigger f,R and smaller

$\tilde{m}, \hat{z}_{1i}$ will make V_{crit} higher, hence safer, and vice versa. Also, by noting that larger $f/\tilde{m}$ requires smaller z_1' relative to $\hat{z}_2$ it follows from Eq. (68) that the radius of the stator and the initial amplitude of the rotor are the most important factors in considering thermoelastic effect. It is noted again that when $\tilde{m}$ approaches zero, there exists no operating first mode wave in the film; same result will occur when initial first mode waviness approaches zero. In both cases, there will be no thermoelastic deformation in the rotor first mode hence no thermoelastic instability. These observations can be reflected from Eq. (69) by noting that V_{crit} approaches infinity and are consistent with the previous theory [4].

RESULTS AND DISCUSSION

For flexibly mounted face seals, if there exists only first mode waviness on the rotor, and axial load is comparable with stator weight, then there will be no admissible steady operation under the assumption of synchronous motion. If there exists only second mode waviness, then thermoelastic instability will not occur [4]. For the case where both first and second mode waviness is present, the condition for steady operation requires $z_1' \ll \hat{z}_2$. It is found that axial load is supported largely by the second mode while the first mode wave will be responsible for the motion of the stator. In such situations, thermoelastic deformation will grow when sliding speed increases. Although it will not reach infinity as in the case of the fixed mounted face seal [1], it may reach a certain value where the requirement of $z_1' \ll \hat{z}_2$ fails. This enables one to determine the critical sliding speed, which will depend on load, mass of stator, radius of stator, initial first mode waviness of the rotor and initial phase angle between first and second mode waviness of the rotor.

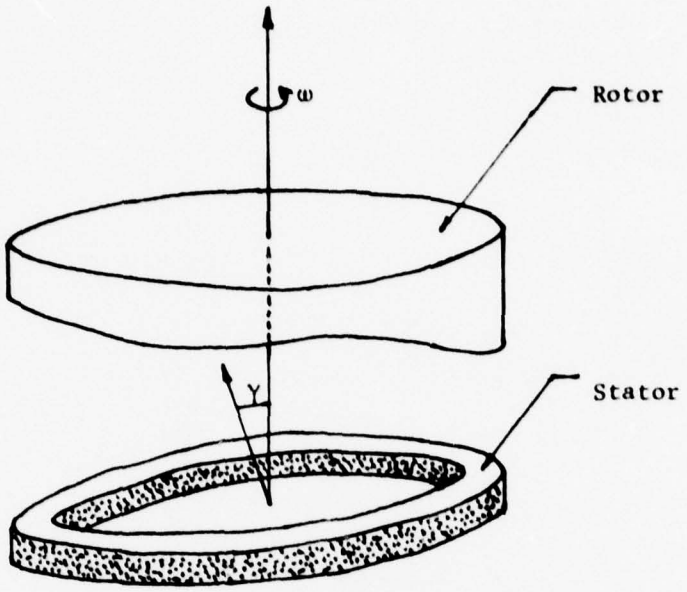

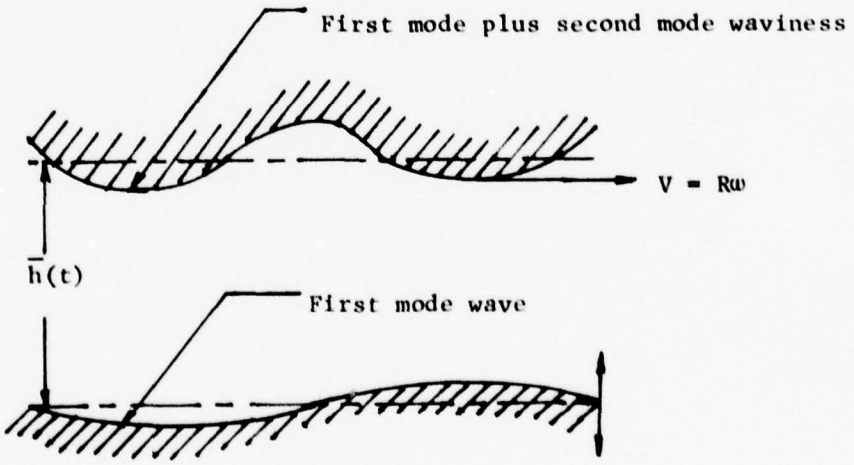

Figure 1. Sketch of Three Degree of Freedom Face Seal Model with Two Modes of Waviness

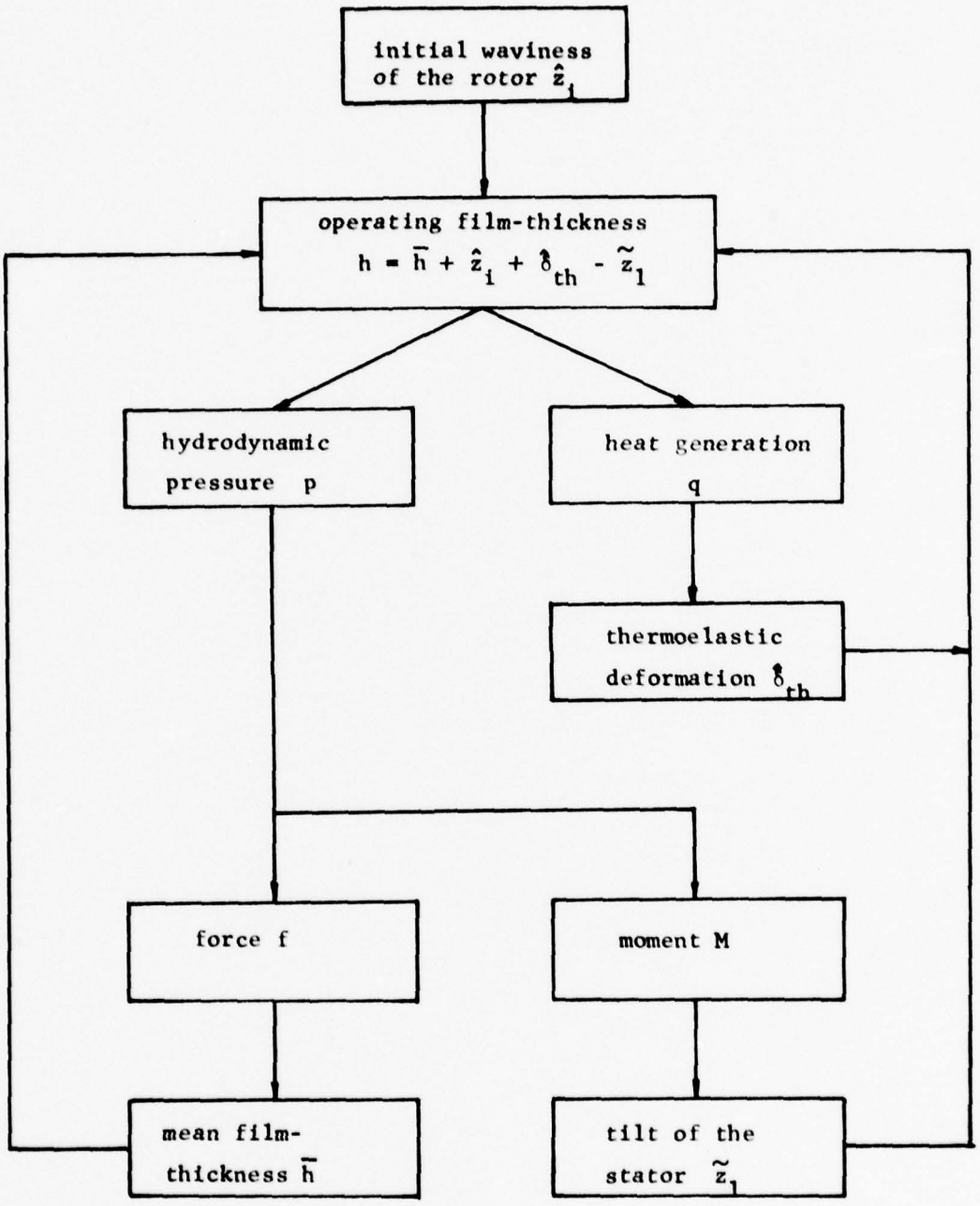

Figure 2. Block Diagram for Thermoelastic Analysis

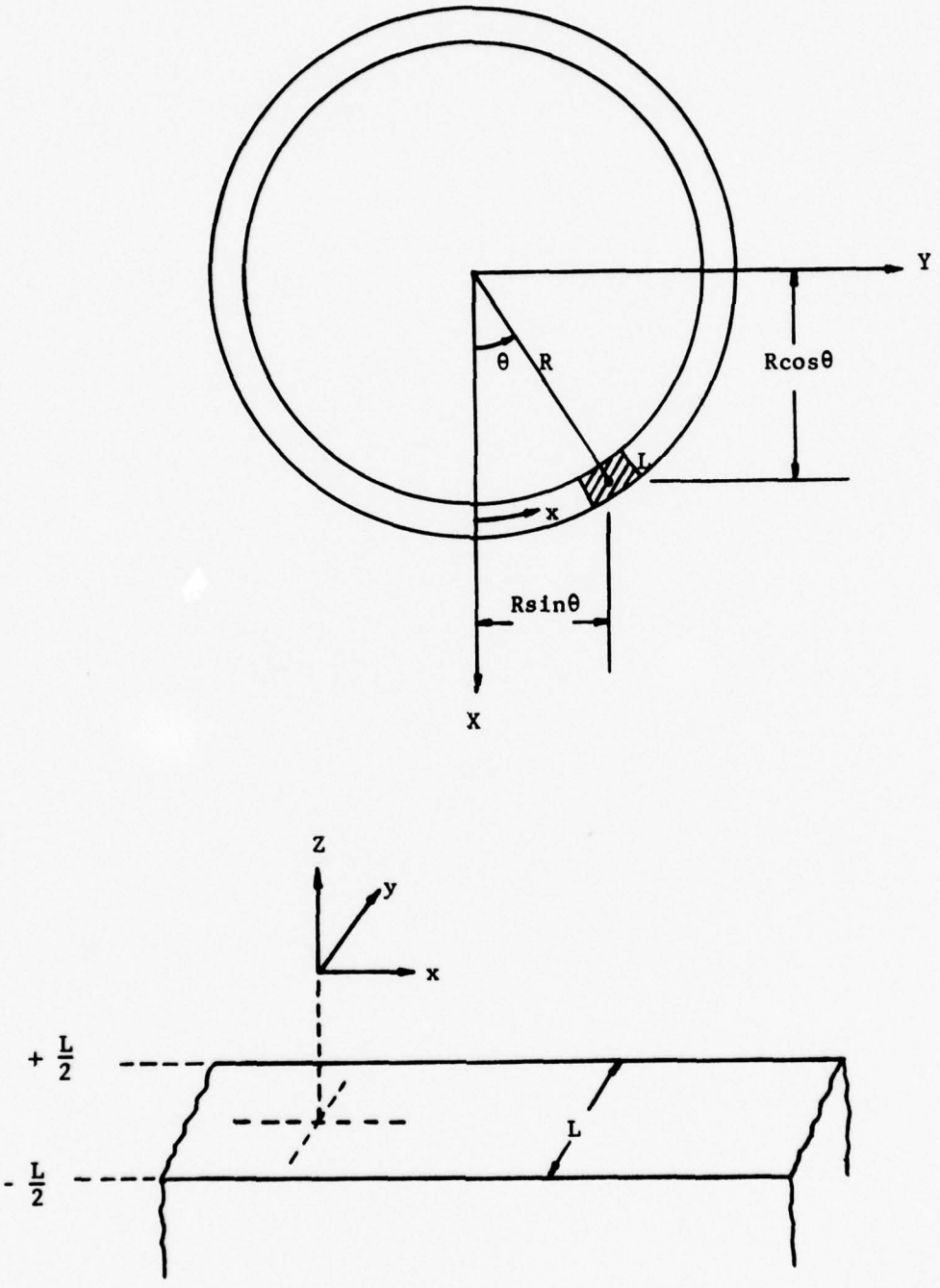

Figure 3. Axes of Coordinates for the Narrow-face Seal

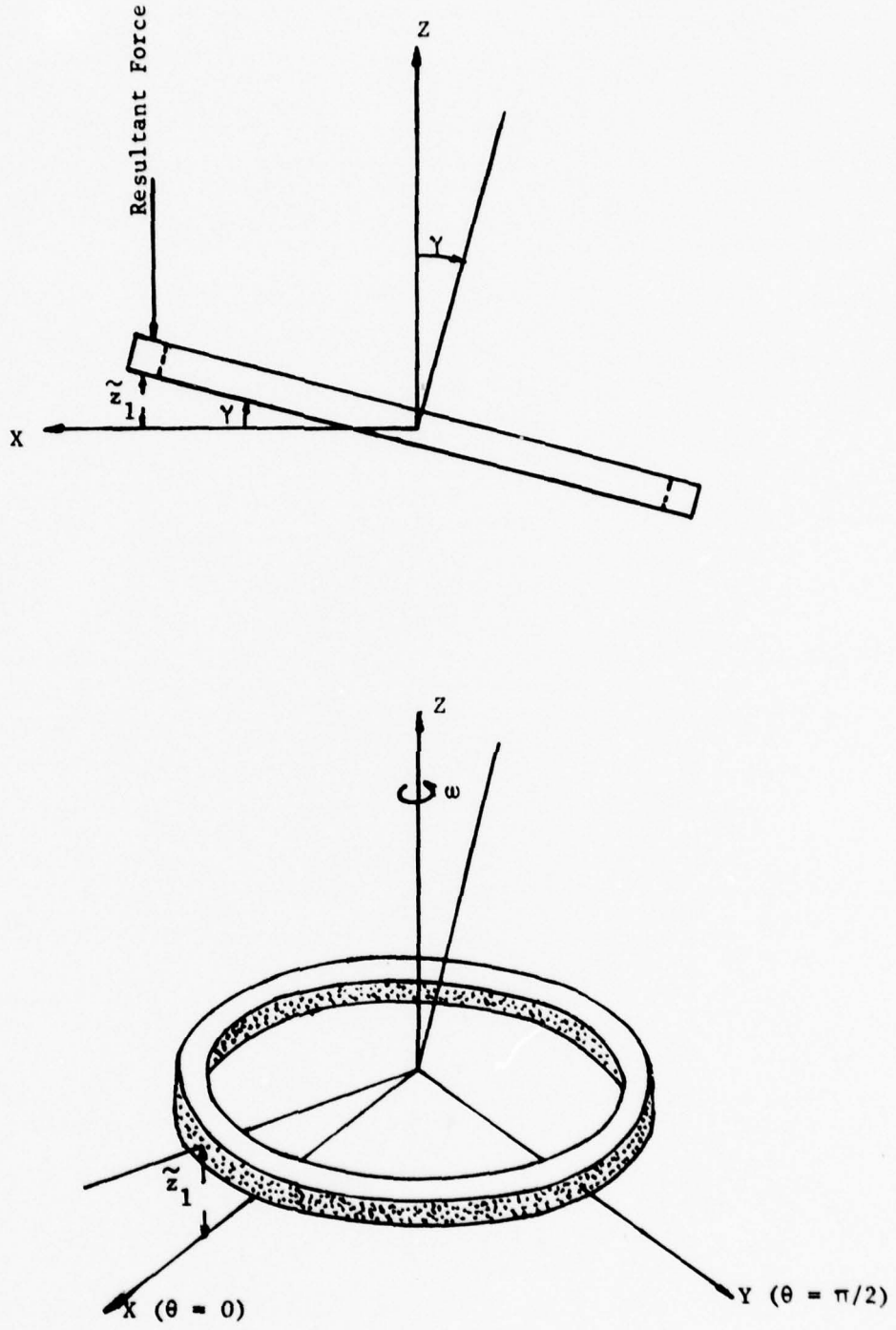

Figure 4. Motion of the Stator and the Definition of Rotating Coordinates

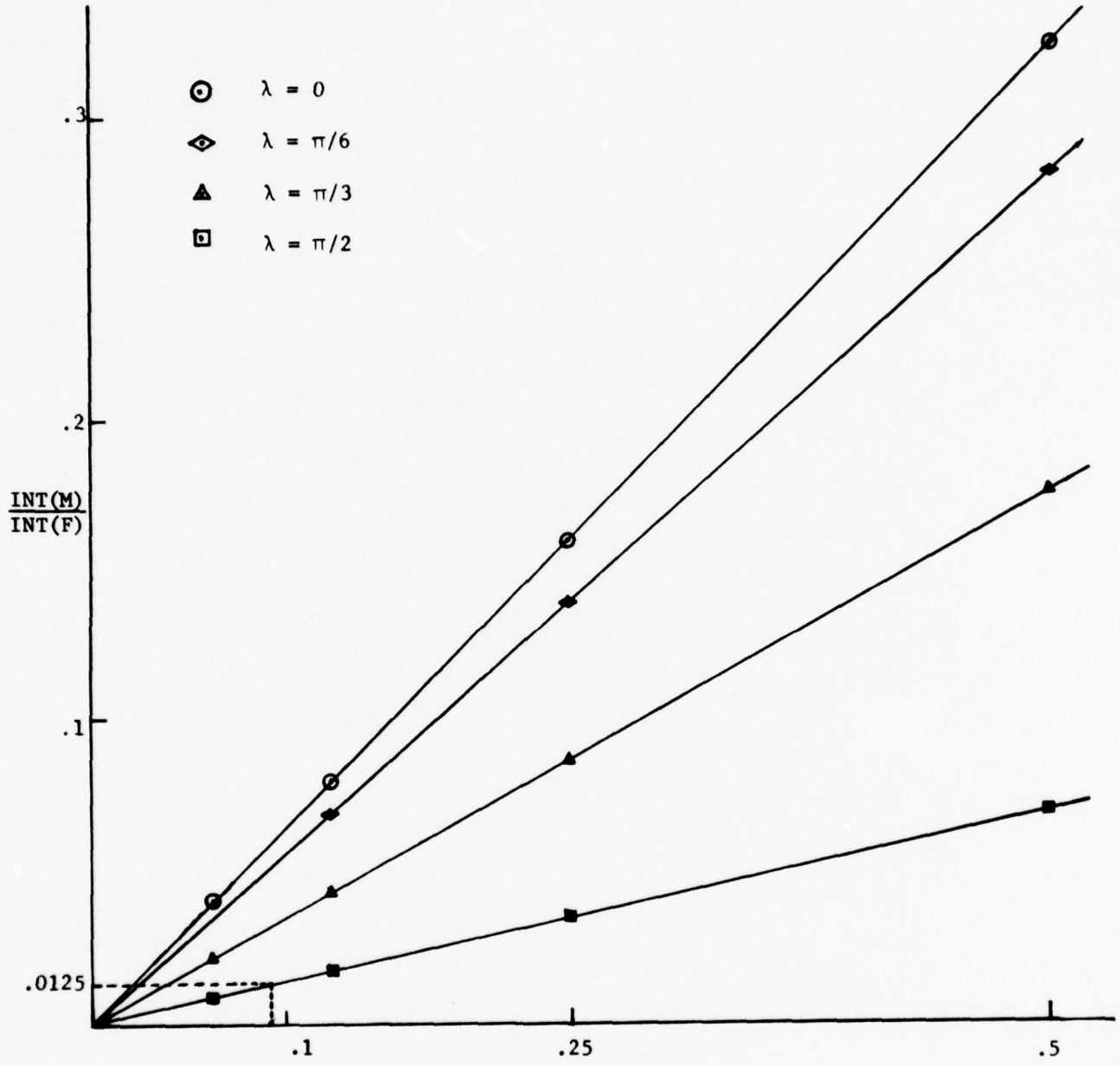

Figure 5. (Moment integral/Force Integral) vs. ζ for small-perturbation Analysis

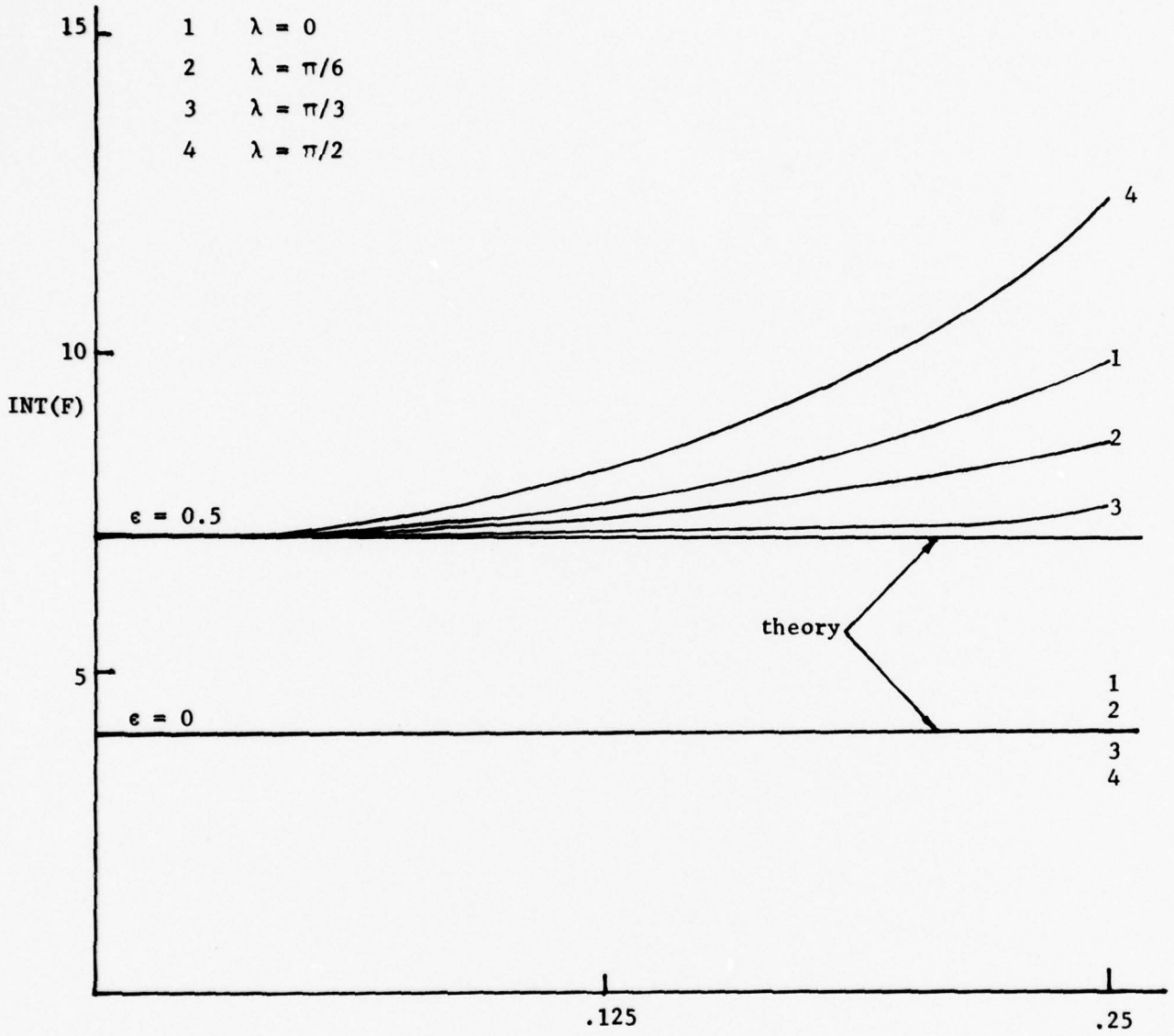

$$\zeta = \frac{\text{amplitude of first mode wave } (z_1')}{\text{amplitude of second mode wave } (\hat{z}_2)}$$

$$\epsilon = \frac{\hat{z}_2}{\bar{h}}$$

Figure 6. Force Integral vs. ζ for Both Small-perturbations (ϵ =0) and Large Amplitude Waviness (ϵ = 0.5)

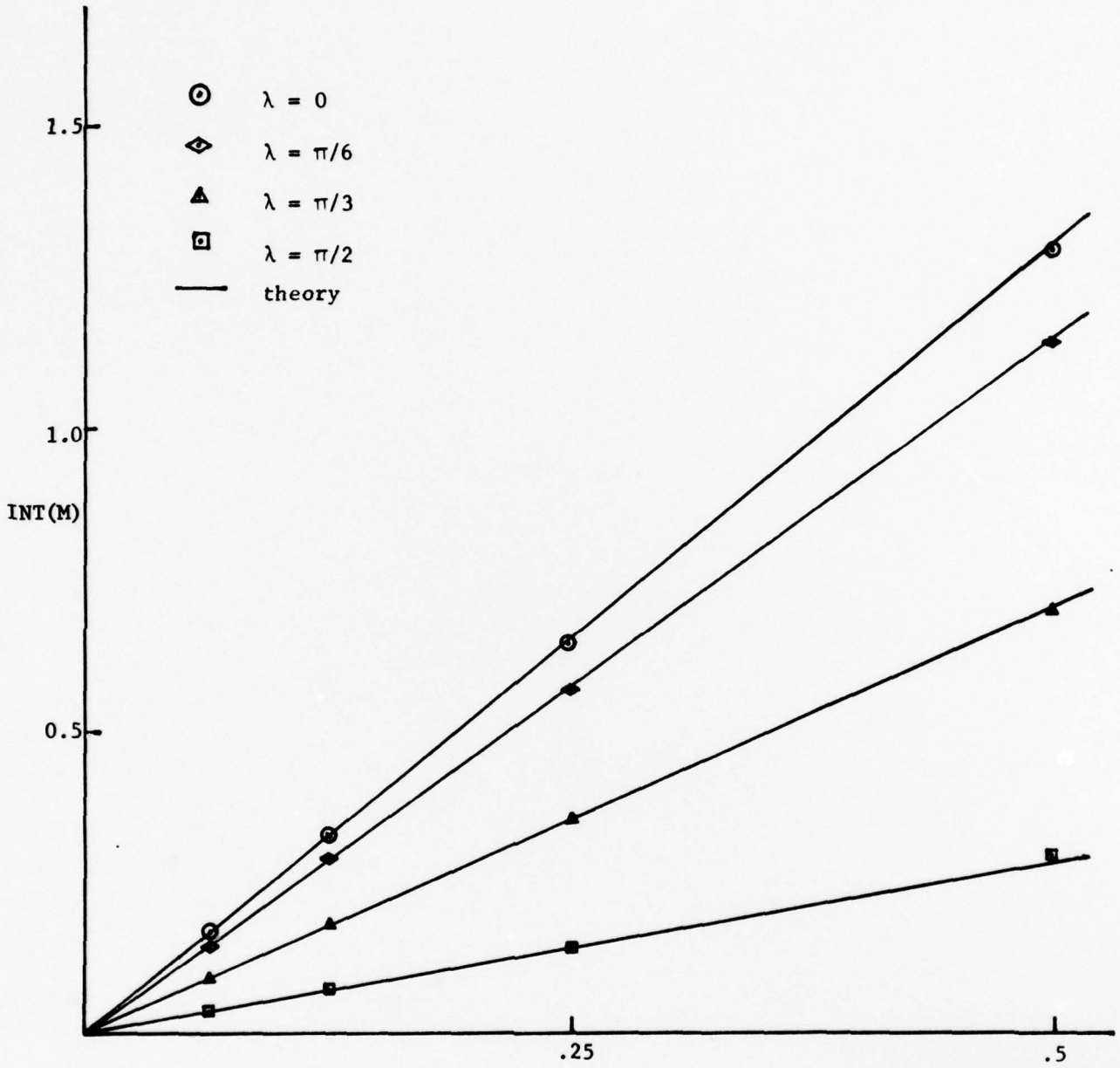

$$\zeta = \frac{\text{amplitude of first mode wave } (z_1')}{\text{amplitude of second mode wave } (z_2'')}$$

Figure 7. Moment Integral vs. ζ for Small-perturbation Analysis

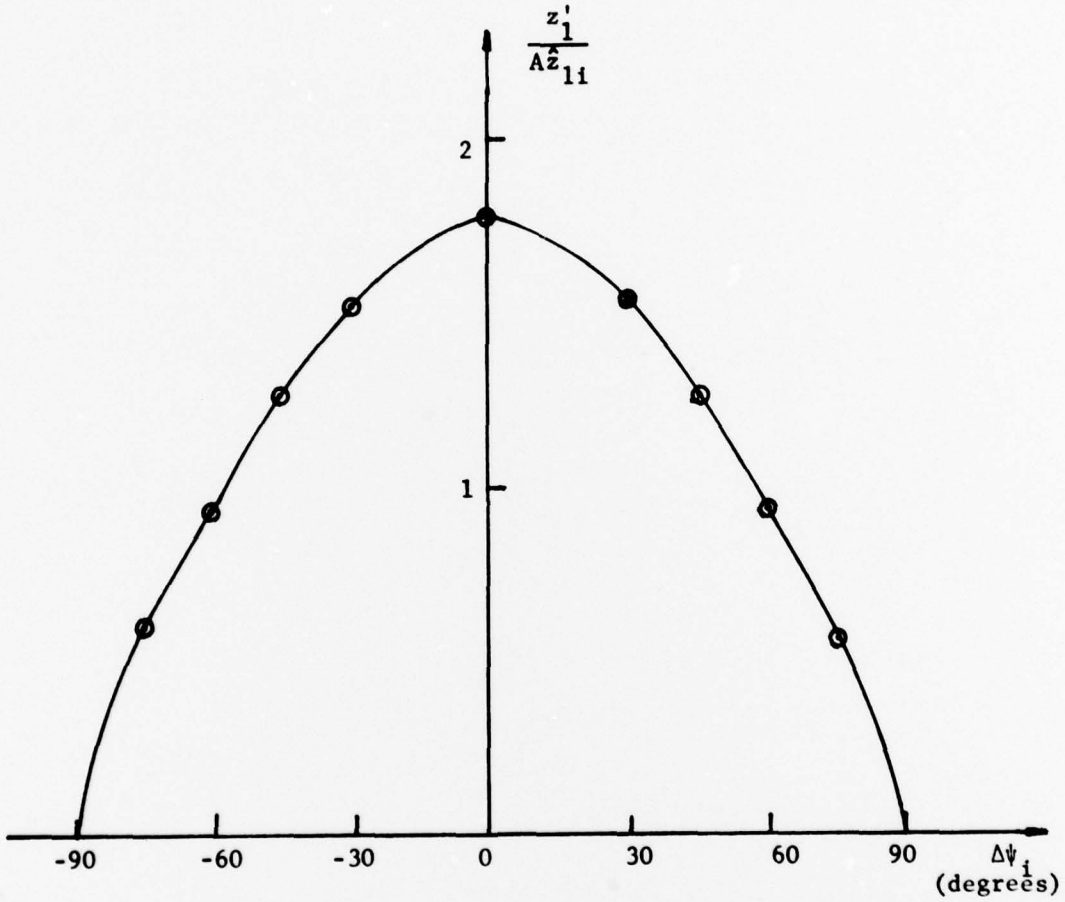

Figure 8. $z_1'/A\hat{z}_{1i}$ vs. $\Delta\psi_i$ at AB = 0

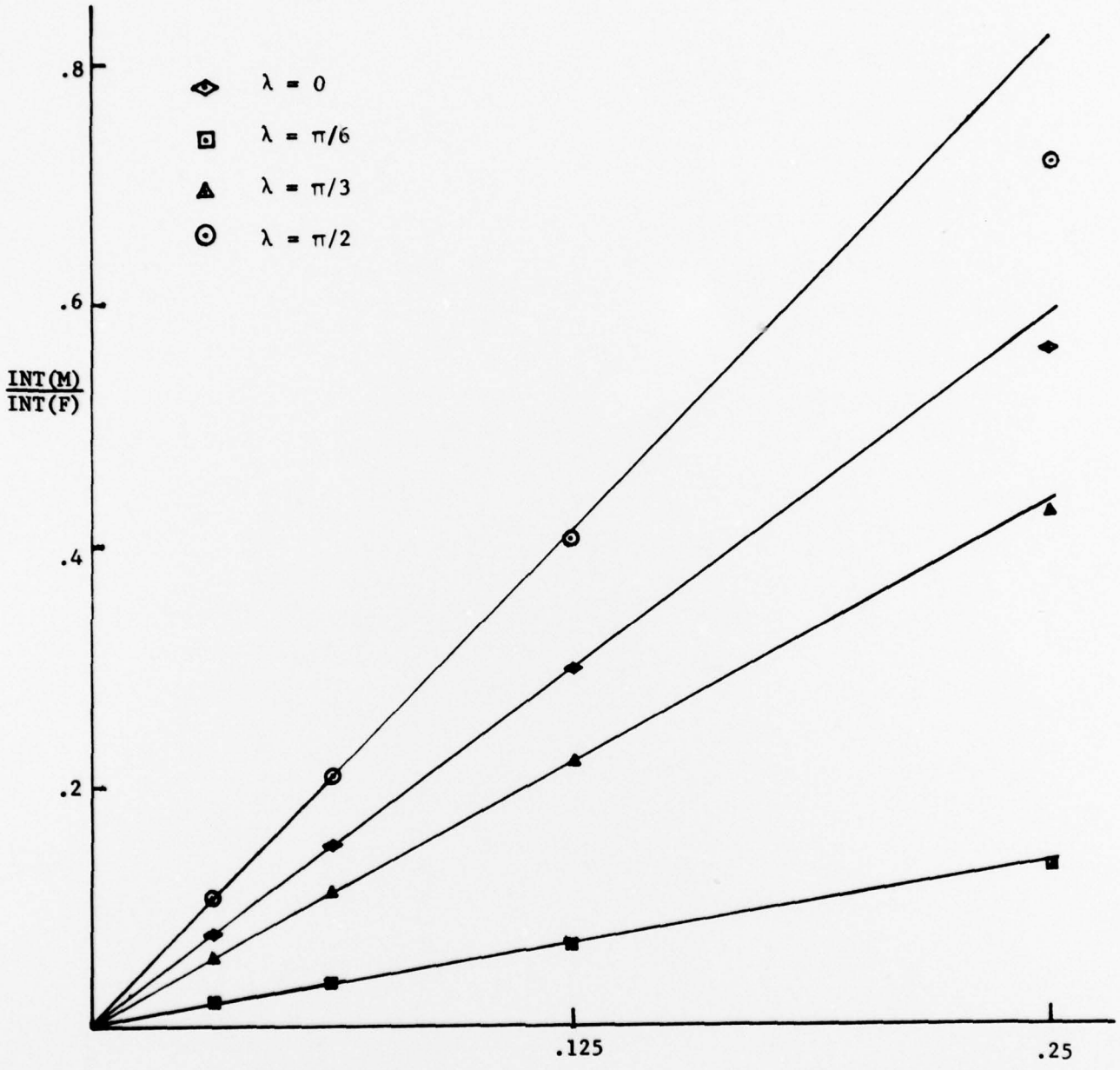

$$\zeta = \frac{\text{amplitude of first mode wave } (z_1')}{\text{amplitude of second mode wave } (\bar{z}_2)}$$

$$\epsilon = \frac{\hat{z}_2}{\bar{h}}$$

Figure 9. (Moment Integral/Force Integral) vs. ζ for Large Amplitude Waviness ($\epsilon = 0.5$)

$\Delta\psi_i$	ϕ_2	Φ_1	AB	$z_1'/A\hat{z}_{1i}$
0	0	0	8.70	1.18
0	45	-32	0.57	1.47
0	86	-3	0.04	1.75
0	94	3	-0.04	1.75
0	135	32	-0.57	1.47
0	180	0	-8.70	1.18
30	30	-23	0.71	1.31
30	56	-3	0.37	1.50
30	86	20	0.05	1.54
30	98	28	-0.10	1.50
30	128	39	-0.80	0.98
30	146	13	-9.50	0.01
60	68	28	0.43	1.00
60	75	32	0.30	1.00
60	86	38	0.09	0.97
60	97	39	-0.20	0.84
60	109	31	-0.64	0.54
60	116	13	-1.10	0.40
90	-244	-40	-1.27	0.45
90	-210	-23	-4.45	0.21
90	0	-180	-39.2	0.03
90	6	8	39.2	0.03
90	38	28	3.35	0.26
90	71	38	0.87	0.47

TABLE 1
Results of Appendix D

Appendix A - Program for computing force and moment integrals

```
      PROGRAM MOMEN ( INPUT,OUTPUT)
      REAL M1,M2,MX1,MX2,MY1,MY2,LAMDA
C     EPSI = 2ND MODE / MEAN FILM THICKNESS
C     ZETA = 1ST MODE / 2ND MODE
      PI=3.1415926
      READ 1,D,ZETA,EPSI
    1 FORMAT(F6.0,F10.8,F3.1)
      DTH=PI/D

      DO 100  I=1,10
      LAMDA=0.
      K=0
      PRINT 2, D,ZETA,EPSI
    2 FORMAT(/,1X,F6.0,F18.8,F10.2)

    3 THETA=-DTH
      MX1=0.
      MX2=0.
      MY1=0.
      MY2=0.
      F1=0.
      F2=0.

    5 THETA=THETA+DTH
      P=ZETA*COS(THETA+LAMDA)+2.*COS(2.*THETA)
      IF( P.LT. 0.  .AND.  THETA .LT. 2.*PI) GO TO 5

      DF1=P*DTH
      F1=F1+DF1
      DMX1=P*SIN(THETA)*DTH
      DMY1=P*COS(THETA)*DTH
      MX1=MX1+DMX1
      MY1=MY1+DMY1

      H=1.+ZETA*SIN(THETA+LAMDA)+EPSI*SIN(2.*THETA)
      HCUBE=H*H*H
      DF2=DF1/HCUBE
      F2=F2+DF2
      DMX2= DMX1/ HCUBE
      DMY2= DMY1/ HCUBE
      MX2=MX2+DMX2
      MY2=MY2+DMY2
      IF(THETA .LT. 2.*PI) GO TO 5

      M1=SQRT(MX1*MX1+MY1*MY1)
      M2=SQRT(MX2*MX2+MY2*MY2)
      FM1=M1/F1
      FM2=M2/F2
      PRINT 50, LAMDA,M1,F1,FM1,M2,F2,FM2
   50 FORMAT(F10.7,6E20.6)
      LAMDA=LAMDA+PI/6.
      K=K+1
      IF(K .LE. 3) GO TO 3
      ZETA=ZETA/2.
  100 CONTINUE
      END
```

Appendix B - Force equation for large amplitude waviness

Recalling that

$$f = \frac{\mu V L^3}{2} \int_{p^+} \frac{1}{h^3} \frac{dh}{d\theta} \, d\theta \tag{1}$$

where

$$h = \bar{h} + z_1' \sin(\theta + \Phi_1) + \hat{z}_2 \sin(2\theta + \phi_2)$$

and p^+ means

$$-\frac{\pi}{4} - \frac{\phi_2}{2} < \theta < \frac{\pi}{4} - \frac{\phi_2}{2} \text{ and } \frac{3\pi}{4} - \frac{\phi_2}{2} < \theta < \frac{5\pi}{4} - \frac{\phi_2}{2}$$

Changing the variable to h, another way to calculate f will be

$$f = \frac{\mu V L^3}{2} \int_{p^+} \frac{1}{h^3} \, dh$$

$$= -\frac{\mu V L^3}{4} \left[\frac{1}{h^2}\right]_{p^+} \tag{2}$$

where p^+ becomes

$$\bar{h} + z_1' \sin(-\frac{\pi}{4} + \lambda) - \hat{z}_2 < h < \bar{h} + z_1' \sin(\frac{\pi}{4} + \lambda) + \hat{z}_2$$

and

$$\bar{h} + z_1' \sin(\frac{3\pi}{4} + \lambda) - \hat{z}_2 < h < \bar{h} + z_1' \sin(\frac{5\pi}{4} + \lambda) + \hat{z}_2$$

where

$$\lambda = \Phi_1 - \frac{\phi_2}{2} \tag{3}$$

Consider only the case $z_1' \ll \hat{z}_2$, where $\hat{z}_2$ not necessarily small compared with $\bar{h}$, then p^+ becomes approximately

$$\bar{h} - \hat{z}_2 < h < \bar{h} + \hat{z}_2$$

and

$$\bar{h} - \hat{z}_2 < h < \bar{h} + \hat{z}_2$$

insertion into Eq. (2) yields

$$f = \mu V L^3 \frac{2\bar{h}\hat{z}_2}{(\bar{h}^2 - \hat{z}_2^2)^2}$$

$$= \frac{2\mu V L^3}{\bar{h}^3} \frac{\hat{z}_2}{(1 - \epsilon^2)^2} \tag{4}$$

where

$$\epsilon = \frac{\hat{z}_2}{\bar{h}}$$

when $\epsilon \approx 0$, Eq. (4) converges to

$$f = \frac{2\mu V L^3}{\bar{h}^3} \hat{z}_2 \tag{5}$$

which is the case for small-perturbation analysis.

Appendix C - Moment equation for large amplitude waviness

Recalling that

$$M_X = \frac{-\mu V L^3 R}{2\bar{h}^3} \int_{p^+} \frac{z_1' \cos(\theta+\Phi_1) + 2\hat{z}_2 \cos(2\theta+\phi_2)}{[1+\zeta\epsilon\sin(\theta+\Phi_1) + \epsilon\sin(2\theta+\phi_2)]^3} \sin\theta d\theta \qquad (1)$$

where

$$\zeta = \frac{z_1'}{\hat{z}_2}$$

and

$$\epsilon = \frac{\hat{z}_2}{\bar{h}}$$

For convenience, write M_X as

$$M_X = \frac{-\mu V L^3 R}{2\bar{h}^3} \left\{ INT(M_1) + INT(M_2) \right\} \qquad (2)$$

where $INT(M_1)$, $INT(M_2)$ denote first and second mode components of the integral in Eq. (1).

Consider $INT(M_1)$, when $\zeta \ll 1$ as assumed, it becomes approximately

$$INT(M_1) = \int_{p^+} \frac{z_1' \cos(\theta+\Phi_1)\sin\theta}{[1+\epsilon\sin(2\theta+\phi_2)]^3} d\theta \qquad (3)$$

where p^+ means

$$-\frac{\pi}{4} - \frac{\phi_2}{2} < \theta < \frac{\pi}{4} - \frac{\phi_2}{2} \text{ and } \frac{3\pi}{4} - \frac{\phi_2}{2} < \theta < \frac{5\pi}{4} - \frac{\phi_2}{2}$$

by changing variable θ to θ' as follows

$$\theta' = 2\theta + \phi_2 + \frac{\pi}{2}$$

The integration interval becomes

$$0 < \theta' < \pi \text{ and } 2\pi < \theta' < 3\pi$$

Eq. (3) can be changed to the following form

$$INT(M_1) = \frac{z_1'}{2}\left\{-\sin\Phi_1 \int_o^{\pi} \frac{d\theta}{[1-\epsilon\cos\theta]^3} + \cos(\Phi_1-\phi_2)\int_o^{\pi} \frac{\cos\theta d\theta}{[1-\epsilon\cos\theta]^3}\right.$$

$$\left.+\sin(\Phi_1-\phi_2) \int_o^{\pi} \frac{\sin\theta d\theta}{[1-\epsilon\cos\theta]^3}\right\} \tag{4}$$

The integrals in Eq. (4) can be carried out [11] by writing

$$\cos\beta = \frac{-\epsilon + \cos\theta}{1-\epsilon\cos\theta} \text{ or } \cos\theta = \frac{\epsilon + \cos\beta}{1+\epsilon\cos\beta} \tag{5}$$

such that

$$d\theta = \frac{(1-\epsilon^2)^{\frac{1}{2}} d\beta}{(1 + \epsilon\cos\beta)}$$

results will be

$$\int_o^{\pi} \frac{d\theta}{(1-\epsilon\cos\theta)^3} = \frac{1+(\epsilon^2/2)}{(1-\epsilon^2)^{5/2}}\pi \tag{6}$$

$$\int_o^{\pi} \frac{\cos\theta d\theta}{(1-\epsilon\cos\theta)^3} = \frac{(3/2)\epsilon\pi}{(1-\epsilon^2)^{5/2}} \tag{7}$$

$$\int_o^{\pi} \frac{\sin\theta d\theta}{(1-\epsilon\cos\theta)^3} = \frac{2}{(1-\epsilon^2)^2} \tag{8}$$

hence

$$INT(M_1) = z_1'\left\{-\frac{\pi\sin\Phi_1}{2}\frac{1+(\epsilon^2/2)}{(1-\epsilon^2)^{5/2}} + \frac{3\pi\cos(\Phi_1-\phi_2)}{4}\frac{\epsilon}{(1-\epsilon^2)^{5/2}}\right.$$

$$\left.+\frac{\sin(\Phi_1-\phi_2)}{(1-\epsilon^2)^2}\right\} \tag{9}$$

when $\epsilon \approx 0$, it converges to

$$INT(M_1) = z_1'\left\{-\frac{\pi}{2}\sin\Phi_1 + \sin(\Phi_1-\phi_2)\right\} \tag{10}$$

which is the same as derived for small-perturbation analysis.

As for integral INT(M_2), the $\zeta\epsilon\sin(\theta+\Phi_1)$ term cannot be neglected, in fact, it is the dominant term in the integral. A closed form solution seems impossible; instead, it will be carried out by series expansion as follows

$$\frac{1}{(1+y)^3} = 1 - 3y + 6y^2 - 10y^3 + 15y^4 - +\ldots. \tag{11}$$

where in this case

$$y = \epsilon[\zeta\sin(\theta+\Phi_1) + \sin(2\theta+\phi_2)]$$

since $\zeta \ll 1$, higher order terms are approximately

$$y^2 = \epsilon^2[2\zeta\sin(\theta+\Phi_1)\sin(2\theta+\phi_2) + \sin^2(2\theta+\phi_2)]$$

$$y^3 = \epsilon^3[3\zeta\sin(\theta+\Phi_1)\sin^2(2\theta+\phi_2) + \sin^3(2\theta+\phi_2)]$$

$$y^n = \epsilon^n[n\zeta\sin(\theta+\Phi_1)\sin^n(2\theta+\phi_2) + \sin^n(2\theta+\phi_2)] \tag{12}$$

It can be shown that, for integer n

$$\int_{p+} \cos(2\theta+\phi_2)\sin^n(2\theta+\phi_2)\sin\theta d\theta = 0$$

$$\int_{p+} \cos(2\theta+\phi_2)\sin^n(2\theta+\phi_2)\cos\theta d\theta = 0$$

By changing variable as in the evaluation of INT(M_1), one finds

$$\begin{aligned}\mathrm{INT}(M_2) = 2z_1' \{ & -3\epsilon\int_{p+}\sin(\theta+\lambda)\cos2\theta\sin\theta d\theta \\ & +12\epsilon^2\int_{p+}\sin(\theta+\lambda)\cos2\theta\sin^2 2\theta\sin\theta d\theta \\ & -30\,\epsilon^3\int_{p+}\sin(\theta+\lambda)\cos2\theta\sin^3 2\theta\sin\theta d\theta +-\ldots\}\end{aligned} \tag{13}$$

where

$$\lambda = \Phi_1 - \frac{\phi_2}{2}$$

The final result, taking only the first three terms, is

$$INT(M_2) = z_1' \left\{-6\epsilon[\cos\Phi_1 - \frac{\pi}{4}\cos(\Phi_1-\phi_2)] + 8\epsilon^2\sin(\Phi_1-\phi_2) - 20\epsilon^3[\cos\Phi_1 - \frac{3\pi}{16}\cos(\Phi_1-\phi_2)] + \ldots\right\} \quad (14)$$

It is clear that $INT(M_2)$ is also a linear function of z_1', and will converge to zero when ϵ approaches zero. From Eq. (2,9,14), the total value will be

$$M_X = \frac{-\mu V L^3 R}{2\bar{h}^3} z_1' \left\{\left[-\frac{\pi}{2}\sin\Phi_1 \frac{1+(\epsilon^2/2)}{(1-\epsilon^2)^{5/2}} + \frac{3\pi\cos(\Phi_1-\phi_2)}{4}\frac{\epsilon}{(1-\epsilon^2)^{5/2}} + \frac{\sin(\Phi_1-\phi_2)}{(1-\epsilon^2)^2}\right] + \left[-6\epsilon(\cos\Phi_1 - \frac{\pi}{4}\cos(\Phi_1-\phi_2)) + 8\epsilon^2\sin(\Phi_1-\phi_2) - 20\epsilon^3(\cos\Phi_1 - \frac{3\pi}{16}\cos(\Phi_1-\phi_2)) + \ldots\right]\right\} \quad (15)$$

M_Y can be obtained in the same way with the following result

$$M_Y = \frac{\mu V L^3 R}{2\bar{h}^3} z_1' \left\{\left[\frac{\pi}{2}\cos\Phi_1 \frac{1+(\epsilon^2/2)}{(1-\epsilon^2)^{5/2}} + \frac{3\pi\sin(\Phi_1-\phi_2)}{4}\frac{\epsilon}{(1-\epsilon^2)^{5/2}} + \frac{\cos(\Phi_1-\phi_2)}{(1-\epsilon^2)^2}\right] + \left[-6\epsilon(\sin\Phi_1 - \frac{\pi}{4}\sin(\Phi_1-\phi_2)) + 8\epsilon^2\cos(\Phi_1-\phi_2) - 20\epsilon^3(\sin\Phi_1 - \frac{3\pi}{16}\sin(\Phi_1-\phi_2)) + \ldots\right]\right\} \quad (16)$$

When $\epsilon \approx 0$, it converges to

$$M_Y = \frac{\mu V L^3 R}{2\bar{h}^3} z_1' \left\{\frac{\pi}{2}\cos\Phi_1 + \cos(\Phi_1-\phi_2)\right\} \quad (17)$$

which is the case for small-perturbation analysis.

Appendix D - Program for determining maximum thermoelastic effects

```
      PROGRAM HEAT  (OUTPUT)
      PI=3.1415926
      DEGRE=57.296038
      PI2=PI/2.
      DEL=-PI2-PI/12.
    1 DEL=DEL+PI/12.
      IF(DEL .GT.  (PI2+.0001))  GO TO 100
      PHI2=-2.*PI-PI/24.
   10 PHI2=PHI2+PI/24.
      TANF1=SIN(PHI2)/(COS(PHI2) -PI2)
      PHI1=ATAN(TANF1)
      SHIFT=PHI2/2.-DEL-PHI1
      PSI=PHI2/2.-DEL
      DELD=DEL*DEGRE
      PHI2D=PHI2*DEGRE
      PHI1D=PHI1*DEGRE
      SHIFD=SHIFT*DEGRE
      PSID=PSI*DEGRE
      ZW1=PI2*SIN(PHI2/2. -DEL) + SIN(PHI2/2.+DEL)
      ZW2=PI2-COS(PHI2)
      ZWAVE=ZW1/ZW2
      FPHAS=COS(PHI1-PHI2) + PI2*COS(PHI1)
      IF(ABS(ZWAVE)  .LT.  .0001) GO TO 15
      AB=COS(PHI2/2.-DEL)*FPHAS/(ZWAVE*COS(PHI1))
      IF(ABS(SIN(PHI1))  .LT. 0.000001) GO TO 10
      C=FPHAS/SIN(PHI1)
      D=AB+C
      ZPRIM=ZWAVE/FPHAS
      IF(ZWAVE .LT. 0.000001)  GO TO 10
   15 PRINT 20,DELD,PHI1D,PSID,ZWAVE,AB,ZPRIM,D
   20 FORMAT(4F14.4,3E20.4)
      IF(PHI2 .GT. (2.*PI-.0001)) GO TO 1
      GO TO 10
  100 CONTINUE
      END
```

Appendix E - Remarks on large amplitude waviness

If the restriction of small-perturbation is removed, which means first mode and second mode waviness as well as stator wave amplitude not necessarily small relative to mean film-thickness, force and moment will be different but not change much if $\hat{z}_2/\bar{h}$ is not very far away from zero.

Following the same procedure as did before, the stator amplitude is found to be

$$z_1 = \left(\frac{g}{2\pi^2}\right)\left(\frac{f}{\tilde{w}}\right)\left(\frac{60}{N}\right)^2\left(\frac{INT(M)}{INT(F)}\right)$$

where

$$INT(M) = \int_p^+ \frac{[\zeta\cos(\theta+\phi_1) + 2\cos(2\theta+\phi_2)]\cos\theta d\theta}{[1+\zeta\epsilon\sin(\theta+\phi_1) + \epsilon\sin(2\theta+\phi_2)]^3}$$

$$INT(F) = \int_p^+ \frac{[\zeta\cos(\theta+\phi) + 2\cos(2\theta+\phi_2)]d\theta}{[1+\zeta\epsilon\sin(\theta+\phi) + \epsilon\sin(2\theta+\phi_2)]^3}$$

$$\epsilon = \frac{\hat{z}_2}{\bar{h}}$$

We can still conclude that $\zeta \ll 1$ in order to keep $\tilde{z}_1$ within practical range [Fig. (9) and Appendix A].

Under the assumption of $z_1' \ll \hat{z}_2$, where $\hat{z}_2$ may be comparable with $\bar{h}$, Appendix B shows that force will be approximately

$$f = \frac{2\mu VL^3}{\bar{h}^3}\frac{\hat{z}^2}{(1-\epsilon^2)^2}$$

Therefore force will be changed by the factor

$$\frac{1}{(1-\epsilon^2)^2}$$

for example, if $\epsilon = 0.3$, force will be 1.2 times compared with small-perturbation case.

Appendix C has derived the moment integrals. Results show that moment is a linear function of z_1', and will not change too much if ϵ is not too big.

Appendix F - Stator motion in Eulerian Coordinates

The formulation of Kupperman (12) has been reviewed, and is felt to be appropriate for small, steadily precessing tilt of the type studied here. If one refers to any advanced dynamics text, one finds the angular velocity vectors, referred to Eulerian axes, to be, using present notation:

$$\Omega_y = -\dot{\gamma}$$

$$\Omega_x = \dot{\theta}\sin\gamma$$

$$\Omega_z = \dot{\theta}\cos\gamma + \dot{\phi}$$

Here $\dot{\theta}$ would correspond to ω the speed of rotation of the rotor and if the stator follows rotor tilt it will be the speed of precession of the stator. The quantity ϕ is the spin of the stator relative to the moving coordinate system and must be such as to keep the absolute $\Omega_z = 0$, if gimbals or O-rings keep the seal ring from rotating. If the tilt angle is fixed (steady precession, no rotation), then $\gamma = 0$. Using this information the only moment is that given in Eq. (10).

REFERENCES

1. Haardt, R., and Godet, M., "Axial Vibration of a Misaligned Radial Face Seal Under a Constant Closure Force," Trans. ASLE, Vol. 18, 1, pp. 55-61.

2. Stanghan-Batch, B., and Iny, E. H., "A Hydrodynamic Theory of Radial-Face Mechanical Seals," J. of Mech. Engg. Sci., Vol. 15, No. 1 (1973), pp. 17-24.

3. Banerjee, B. N., "Thermoelastic Effects in the Parallel Sliding of Solid Surfaces Separated by a Viscous Liquid Film," Dissertation (1977), Northwestern University, Evanston, Illinois.

4. Banerjee, B. N., and Burton, R. A., "Thin-Film Flows with Thermoelastically Deformed Boundaries," submitted to I. Mech. E., London.

5. Banerjee, B. N., and Burton, R. A., "Experimental Studies on Thermoelastic Effects in Hydrodynamically Lubricated Face Seals," accepted for publication, ASME Trans., Ser. F.

6. Burton, R. A., "The Role of Insulating Surface Film in Frictionally Excited Thermoelastic Instability," Wear, Vol. 24, No. 2, pp. 189-198.

7. Etsion, I., "The Accuracy of the Narrow Seal Approximation in Analyzing Radial Face Seals," ASLE Paper 78-LC-2B-2, presented at the ASME-ASLE Lubrication Conference, Oct., 1978.

8. Banerjee, B. N., and Burton, R. A., "An Instability for Parallel Sliding of Solid Surfaces Separated by a Viscous Liquid Film," Trans. ASME, JOLT (Jan. 1976), pp. 157-166.

9. Georgopoulos, E., M.S. Thesis (1976), Northwestern University, Evanston, IL.

10. Burton, R. A., Kilaparti, S. R., and Nerlikar, V., "A Limiting Stationary Configuration with Partially Contacting Surfaces," Wear, Vol. 24, No. 2, (1973), pp. 546-551.

11. Cameron, C., "The Principles of Lubrication," John Wiley and Sons, Inc., New York, NY, 1966.

12. Kupperman, David S., "Dynamic Tracking of Non Contacting Face Seals," ASLE Trans., 18 (1975), pp. 306-311.